molecular pharmaceutics

ARTICLE

pubs.acs.org/molecularpharmaceutics

Capping Methotrexate α-Carboxyl Groups Enhances Systemic Exposure and Retains the Cytotoxicity of Drug Conjugated PEGylated Polylysine Dendrimers

Lisa M. Kaminskas,[†] Brian D. Kelly,[‡] Victoria M. McLeod,[†] Gian Sberna,[‡] Ben J. Boyd,[†] David J. Owen,[‡] and Christopher J. H. Porter*[,†]

[†]Drug Delivery, Disposition and Dynamics, Monash Institute of Pharmaceutical Sciences, Monash University, 381 Royal Parade, Parkville, VIC, Australia, 3052

[‡]Starpharma Holdings Ltd, Level 6, Baker Heart Research Building, Commercial Road, Melbourne, VIC, Australia, 3004

Supporting Information

ABSTRACT: A generation 5 PEGylated (PEG 1100) polylysine dendrimer, conjugated via a stable amide linker to OtBu protected methotrexate (MTX), was previously shown to have a circulatory half-life of 2 days and to target solid tumors in both rats and mice. Here, we show that deprotection of MTX and substitution of the stable linker with a matrix metalloproteinase (MMP) 2 and 9 cleavable linker (PVGLIG) dramatically increased plasma clearance and promoted deposition in the liver and spleen (50−80% of the dose recovered in the liver 3 days post dose). Similar rapid clearance was also seen using a scrambled peptide suggesting that clearance was not dependent on the cleavable nature of the linker. Surprisingly, dendrimers where OtBu capped MTX was linked to the dendrimer surface via the hexapeptide linker showed equivalent in vitro cytotoxicity against HT1080 cells when compared to the uncapped dendrimer and also retained the long circulating characteristics of the stable constructs. The OtBu capped MTX conjugated dendrimer was subsequently shown to significantly reduce tumor growth in HT1080 tumor bearing mice compared to control. In contrast the equivalent dendrimer comprising uncapped MTX conjugated to the dendrimer via the same hexapeptide linker did not reduce tumor growth, presumably reflecting very rapid clearance of the construct. The results are consistent with the suggestion that protection of the α-carboxyl group of methotrexate may be used to improve the circulatory half-life and reduce the liver accumulation of similar MTX-conjugated dendrimers, while still retaining antitumor activity in vivo.

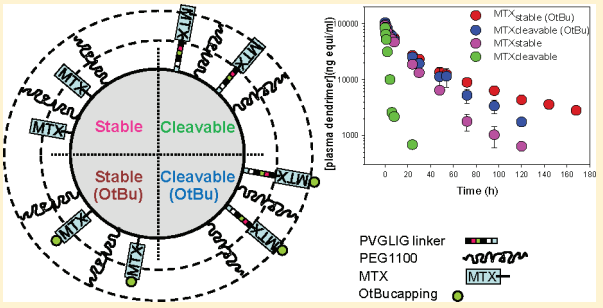

KEYWORDS: dendrimer, modified methotrexate, pharmacokinetics, matrix metalloproteinase cleavable, alpha-carboxyl protection

INTRODUCTION

Nanoparticulate and colloidal drug delivery systems have been documented as a possible means of improving the delivery of chemotherapeutic drugs to solid tumors and at the same time reducing drug exposure to noncancerous tissue.[1,2] This ability is unique to nanosized material and is afforded by characteristics inherent in solid tumors. Specifically, the continuous vascular endothelium present in noncancerous tissue is characterized by the presence of tight junctions between adjacent endothelial cells and an underlying basement membrane that together form a considerable barrier to the extravasation of high molecular weight materials such as proteins and colloids.[3] In contrast, the vascular architecture in tumors is considerably more permeable due to the presence of wider intercellular spaces and an incomplete basement membrane.[3] Furthermore, the extracellular space in normal tissue is drained by lymphatic capillaries which have much larger interendothelial junctional distances than the vascular endothelium and also lack a basement membrane, properties that together serve to promote the drainage of high molecular weight molecules, cellular debris and foreign cellular material such as invading pathogens into the lymph.[4] The material drained into the lymph is subsequently presented to the immune system and lymph nodes and eventually removed by filtration and phagocytosis.[4] Solid tumors, however, lack a functioning lymphatic system, which, in combination with the more permeable blood vasculature, enables enhanced access and reduced clearance of nanosized material.[5,6] This phenomenon is termed the enhanced permeation and retention (EPR) effect and occurs specifically in tissues with compromised vasculature and reduced lymphatic drainage. Several nanosized colloidal systems (including liposomes,[7,8] polymers,[9−11] nanoparticles[12,13] and dendrimers[14−19])

Received: June 1, 2010
Accepted: December 20, 2010
Revised: November 5, 2010
Published: December 20, 2010

have therefore been examined as potential drug delivery systems and have shown improved chemotherapeutic efficacy in solid tumors. A further potential advantage of nanosized delivery systems is the capacity to reduce the multidrug resistance properties of some tumors by facilitating drug uptake into the tumor via alternate (typically endocytic) routes.[20,21]

Drug loading of nanosized drug delivery systems may be via noncovalent entrapment within a hydrophobic core (as is commonly seen in liposomes, micelles and some dendritic systems) or via covalent conjugation to functional groups (such as those present on linear and dendritic polymers and on the surface of nanoparticles or liposomes).[22,23] A disadvantage of noncovalent entrapment is the potential for nonspecific drug release and gradual leakage of drug from the delivery systems over time.[16] In contrast, covalent conjugation reduces the potential for nonspecific release and also attenuates the potential for gradual leakage of drug from the delivery systems. Drug conjugation can be achieved using chemical linkers designed to be cleaved in the presence of enzymes in the environment of the tumor or in lysosomes or under microenvironmental conditions that are specific to the tumor. For example, pH labile esters[19] and hydrazones[17] have been suggested to facilitate the release of drug within the acidic microenvironment of many solid tumors and have been employed in a number of nanoparticulate delivery systems.

Alternatively, the selective overexpression by invasive solid tumors of enzymes responsible for basement membrane degradation and matrix remodeling may be utilized as a means of selective liberation of covalently bound drug.[10,24,25] For example, Chau and colleagues have identified a peptide sequence that is cleaved specifically by matrix metalloproteinases (MMP) 2 and 9.[10,24] The inactive precursors to matrix metalloproteinases are normally constitutively expressed in tissues; however, in many invasive tumors MMPs are overexpressed. Using this approach, Chau et al. showed that liberation of methotrexate (MTX)-PVG from a 70 kDa dextran containing a Pro-Val-Gly-Leu-Ile-Gly (PVGLIG) linker to methotrexate was possible in the presence of MMP2 and MMP9. In spite of the reduced in vitro cytotoxicity of the modified drug (i.e., MTX-PVG) the authors reported improved in vivo antitumor efficacy of the MTX-PVGLIG-dextran construct on account of better targeting of the macromolecular construct to HT1080 tumors followed by drug liberation in the tumor environment.[10]

Previous studies have described the tumor targeting and anticancer activity of MTX conjugated PAMAM[19] and polylysine[18] dendrimers, providing encouraging evidence of the potential of this approach to provide for improved cytotoxic drug delivery systems. In previous studies from this laboratory the pharmacokinetics, organ biodistribution and tumor targeting of a series of PEGylated, MTX-conjugated dendrimers have been evaluated, and for the largest G5 dendrimer (which contained conjugated PEG chains of 1100 Da), a construct with a long circulatory half-life ($t_{1/2}$ ~ 2 days) and high tumor uptake (1−2%/g and 5−10-fold higher than control tissues) was possible.[18] In these studies MTX was deliberately conjugated to the dendrimer using a stable linker with potential interaction sites for MTX (e.g., folate and reduced folate transport systems) blocked using an O-*t*-butyl(OtBu) capping group. This approach was taken in order to isolate the instrinsic organ distribution and tumor targeting properties of the dendrimer rather than complicating data interpretation with the prospect of interaction with MTX receptors or transport proteins or drug liberation and subsequent biodegradation of the complex.

Table 1. Chemical Properties of Generation 5 MTX Conjugated Dendrimers[a]

	MW (kDa)	% MTX by wt	radioactivity (μCi/mg)
SPN dendrimers			
$MTX_{cleavable}$	64.7	20	0.483
$MTX_{cleavable}$(OtBu)	64.0	20	0.795
MTX_{stable}	51.9	26	0.331
LYS dendrimers			
$MTX_{cleavable}$	68.5	17	0.525
$MTX_{cleavable}$(OtBu)	70.9	17	0.653

[a] MW and % MTX by weight were determined by MALDI MS. For details of ^{1}H NMR and MS characterization see the Supporting Information.

The current study therefore planned to extend these studies to incorporate an MMP-labile linker into the design of the previous MTX−dendrimer complex and to evaluate efficacy in a rodent tumor model. As part of these studies, the OtBu capping group was also removed from the conjugated MTX and surprisingly this led to a profound change in the systemic clearance of the complex and a rapid uptake of the dendrimer into the liver. The focus of the current studies were therefore expanded to explore in more detail the potential pharmacokinetic and cytotoxic consequences of the inclusion of the OtBu capping group in comparison to the unprotected complex (since the pharmacokinetic profile of the capped construct appeared to provide advantage). Previous studies also suggest that pharmacokinetic advantage may be provided by the utilization of a synthetic analogue of lysine (succinimyldipropyldiamine, SPN) in the outer layer of the dendrimer,[18] and therefore the initial pharmacokinetic studies were also conducted using SPN and Lys derived dendrimers.

METHODS

Materials. Buffer reagents were purchased from Aldrich and were used without further purification. Tripeptide Pro-Val-Gly (PVG) and hexapeptides (PVGLIG and LPGVIG) were purchased from EZbiolab (Carmel, IN, USA). Methotrexate (MTX), sterile L-glutamine, penicillin−streptomycin (pen/strep), nonessential amino acids (NEAA), Hanks balanced salt solution (HBSS), trypsin-EDTA, 3-[4,5-dimethylthiazol-2-yl]-2,5-diphenyltetrazolium bromide (MTT) and Eagle's minimum essential medium with Earle's salts (MEM) were purchased from Sigma (NSW, Australia). Horse serum, fetal bovine serum (FBS), Matrigel and 75 cm^3 flasks were purchased from Gibco (Invitrogen, VIC, Australia). Microplates (96 well flat clear bottomed) and 6 well plates were from Greiner Bio-One (Biolab, VIC, Australia). Matrix metalloproteinase 2 and 9 were from Calbiochem (Merck Biosciences, VIC, Australia). Unlabeled lysine for synthesis was purchased from Bachem (Bunbendorf, Switzerland). (L)-(4,5-^{3}H)-Lysine (1 mCi/mL) was purchased from MP Biomedicals (Irvine, CA, USA). HT1080 cells were purchased from ECACC (Salisbury, U.K.). Monodisperse PEG_{1100}NHS were purchased from Quanta BioDesign, Ltd. (USA). Soluene-350 and Starscint were purchased from Packard Biosciences (Meriden, CT). Heparin (10,000 U/mL) was from Faulding (SA, Australia). Saline was from Baxter Healthcare (NSW, Australia). All other chemicals were HPLC grade and were used without any further purification.

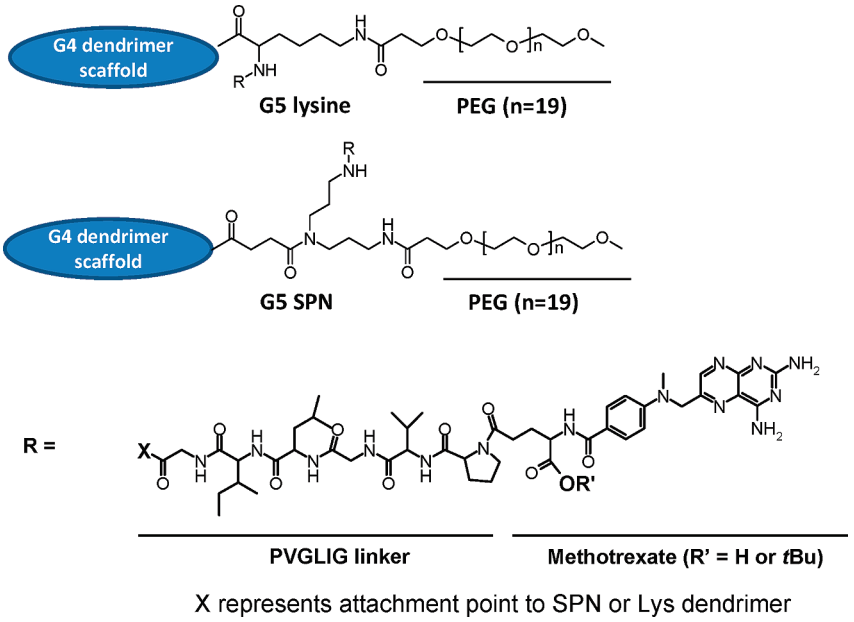

Figure 1. Structure of the surface of cleavable MTX-conjugated dendrimers containing outer scaffolds of L-lysine or SPN. The G4 dendrimer scaffold is composed entirely of lysine, and the G4 layer contains the ^{3}H-label. R represents the structure of the MTX-PVGLIG function, and R′ on methotrexate is either H or *t*Bu.

Synthesis and Characterization of Radiolabeled Dendrimers. Purified MTX-PVG and OtBu-MTX-PVG (for standard curve generation) were prepared as previously described.[26] A series of generation 5 poly-L-lysine dendrimers were prepared where tritium radiolabel was incorporated using a lysine moiety that contains tritium labels at the γ and δ positions in the outer natural lysine layer.[27] A succinimyldipropyldiamine (SPN) wedge (prepared as previously reported[18]) containing 50% MTX and 50% PEG_{1100} was then conjugated to the polylysine core to produce three generation 5 dendrimers containing 50% PEG_{1100} and 50% MTX bound to surface amines via either a stable (amide) or cleavable (hexapeptide, Figure 1) spacer as described previously.[18,26] Additionally, two dendrimers were prepared which contained a surface of 50% MTX and 50% PEG_{1100} attached directly to an all L-lysine G5 scaffold as described previously.[28] Final products were characterized by MALDI MS, ^{1}H NMR and HPLC−UV as described previously[28] (see Supporting Information). The dendrimer nomenclature used for fully PEGylated and stable MTX-conjugated dendrimers has been described elsewhere.[18] The chemical properties of the synthesized dendrimers are given in Table 1 and dendrimer nomenclature is summarized in Table 2.

The specific radioactivity of the dendrimers was determined by dilution of a known mass of dendrimer in 1 mL of Starscint, followed by scintillation counting using a Packard Tri-Carb 2000CA liquid scintillation analyzer (Meriden, CT). Specific activity was typically within the range of 0.3 to 1 μCi/mg.

MMP Mediated Cleavage of MTX-PVG and OtBu-MTX-PVG from $MTX_{cleavable}$ Dendrimers. The cleavage of MTX-PVG or OtBu-MTX-PVG from the $MTX_{cleavable}$ dendrimers was measured in triplicate using a previously reported method.[26] Briefly, stock solutions of MMP2 and 9 were diluted to approximately 270 nM in storage buffer (50 mM HEPES, 10 mMCaCl2, 20% glycerol, 0.005% BRIJ 35, pH 7.5) and stored in 11 μL aliquots at −80 °C until required. Dendrimer (5 μM) was prepared in reaction buffer (50 mM TRIS base, 0.2 M NaCl, 10 mM CaCl2, pH 7.5) in 250 μL PCR tubes and prewarmed to 37 °C in a water bath. Reactions were initiated by the addition of 4.6 μL of stock MMP to give a final protein concentration of 5 nM. Reaction samples (20−50 μL) were taken at 1 and 24 h and quenched with ice cold 40 mM EDTA to give a final volume of 100 μL. Ninety microliter aliquots of these were then injected onto the HPLC for analysis of MTX-PVG or OtBu-MTX-PVG as described below.

Stability of $MTX_{cleavable}$ Dendrimers in Plasma. The stability of the PVGLIG-linker contained in the $MTX_{cleavable}$ (including cleavable systems containing OtBu-MTX) dendrimers was determined by incubation of 100 μg of dendrimer in 1 mL of fresh rat plasma at 37 °C for up to 3 days. At 48 and 72 h, 500 μL aliquots were collected and analyzed for MTX-PVG or OtBu-MTX-PVG as described below. MTX-PVG or OtBu-MTX-PVG was extracted by addition of 1 volume of acetonitrile followed by centrifugation at 5000*g* for 10 min at 4 °C. The supernatant was then dried under nitrogen at 60 °C for 1 h and reconstituted in 200 μL of mobile phase. A 100 μL aliquot was then injected onto the HPLC.

Cell Culture. HT1080 cells (that overexpress MMP2 and 9) were maintained in MEM supplemented with 2 mM L-glutamine, 1% pen/strep, 1% NEAA and 10% FBS in a humidified 5% CO_2 atmosphere at 37 °C. Cells were passaged using trypsin-EDTA three times per week and were used between passages 5 and 10.

Cytotoxicity of MTX, MTX-PVG, OtBu-MTX-PVG and MTX Conjugated Dendrimers on HT1080 Cells. HT1080 cells were seeded in each well of two 96 well microplates in 100 μL of serum containing medium at a density of 10,000 cells per well. After 24 h, the medium was exchanged to serum free medium containing supplements as described above. Free MTX, MTX-PVG, OtBu-MTX-PVG, *t*-butanol or MTX dendrimer (0.001 to 500 μM MTX equivalents) was then added to triplicate wells and incubated for 48 h. MTT solution (10 μL) was then added to each well and incubated at 37 °C for a further 2 h. The medium was removed from each well and replaced with 100 μL of dimethyl sulfoxide. Microplates were vortex mixed briefly before the color intensity was read in a Fluorostar microplate reader (Bio-Strategy, Auckland, NZ) at 540 nm. The percent of viable

Table 2. Dendrimer Nomenclature

SPL number	Chemical composition	Abbreviated notation
SPL-8108	$BHALys[Lys]_{16}[SuN(PN)_2(PEG_{1100})(GILGVP\text{-}MTX)]_{32}$	$SPN\text{-}MTX_{cleavable}$
SPL-8153	$BHALys[Lys]_{16}[SuN(PN)_2(PEG_{1100})(GILGVP\text{-}MTX\text{-}OtBu)]_{32}$	$SPN\text{-}MTX_{cleavable}(OtBu)$
SPL-8152	$BHALys[Lys]_{16}[SuN(PN)_2(PEG_{1100})(MTX)]_{32}$	$SPN\text{-}MTX_{stable}$
SPL-8021	$BHALys[Lys]_{16}[SuN(PN)_2(PEG_{1100})(MTX\text{-}OtBu)_{32}$	$SPN\text{-}MTX_{stable}(OtBu)$
SPL-8301	$BHALys[Lys]_{32}[(PEG_{1100})(GILGVP\text{-}MTX)]_{32}$	$Lys\text{-}MTX_{cleavable}$
SPL-8300	$BHALys[Lys]_{32}[PEG_{1100})(GILGVP\text{-}MTX\text{-}OtBu)]_{32}$	$Lys\text{-}MTX_{cleavable}(OtBu)$

cells relative to untreated control cells was determined by the equation $(A_s - A_b)/(A_c - A_b) \times 100$ where A_s is the absorbance of the sample, A_b is absorbance of blank cells not treated with MTT solution and A_c is the absorbance of untreated control cells. IC_{50} values were determined by fitting the data to a variable slope sigmoidal dose response curve ($Y = 100/(1 + 10^{[LogIC50-X](Hill\ slope)})$) in GraphPad Prism V4.0 (La Jolla, CA, USA).

In Vitro Cleavage of MTX-PVG and OtBu-MTX-PVG from $MTX_{cleavable}$ Dendrimers by Cultured HT1080 Cells. HT1080 cells were plated in serum-containing MEM (2 mL) at a density of 250,000 cells per well in triplicate in 2 cm culture dishes. Cells were allowed to adhere overnight. The medium was then changed to 1 mL of serum free MEM per well and approximately 1 μM of dendrimer (equivalent to 32 μM MTX equivalents) added and incubated for a further 48 h. Control wells ($n = 3$) contained 1 mL of serum free MEM and 32 μM MTX equivalents of dendrimer without cells. Cells were then scraped from the wells and medium + cells collected and sonicated at 50 Hz for 5 min. MTX-PVG or OtBu-MTX-PVG was extracted from the cell suspension or cell-free medium and assayed using the HPLC method described for medium below.

Animals. Rats (male, Sprague−Dawley, 270−350 g) and mice (female, Balb/c *nu/nu*, 6 weeks) were supplied by animal services at Monash University and were maintained on a 12 h light/dark cycle and fed standard rodent show. Food and water were provided to rats ad libitum prior to surgery. Food was withheld after surgery and 8 h after administration of the iv dose, but water was available at all times. Food was provided at all other times. All animal experiments were approved by the Victorian College of Pharmacy Animal Ethics Committee, Monash University (Melbourne, Victoria).

Determination of Intravenous Plasma Pharmacokinetics. Rats were cannulated via the right jugular vein and carotid artery under isoflurane anesthesia as described previously.[27] After surgery, rats were transferred to metabolism cages and were allowed to recover overnight prior to administration of 1 mL of dendrimer solution (in sterile saline) via the jugular vein cannula to provide a final dose of 5 mg/kg. Prior to dosing, a blank blood sample (150 μL) was collected via the carotid artery cannula into a heparinized (100 U) Eppendorf tube. Animals were dosed with each dendrimer as a bolus over 1.5 min. Dendrimer remaining in the cannula was flushed through with a further 200 μL of heparinized saline (2.5 U heparin/mL) over an additional 30 s, after which a zero time point sample (150 μL, $t = 0$) was collected via the carotid artery cannula to facilitate estimation of C_p^0 and V_c. Further blood samples were collected at $t = 0$, 10, 20, 30, 45, 60, 90, 120, 180, 240, 360, 480, 1440, 1800 min and at 48, 54, 72, 78, 96, 102, and 120 h. Whole blood samples were centrifuged (3500*g*) for 5 min to isolate plasma. Plasma samples (50−100 μL) were then mixed with 1 mL of Starscint in 6 mL scintillation vials and counted for ^{3}H-content.

Excretion of Injected Radiolabel and Biodistribution. Urine was collected and analyzed for ^{3}H-content over time periods 0−8, 8−24, 24−48, 48−72, 72−96 and 96−120 h. Aliquots (100−200 μL) of urine collected over these time periods were analyzed for tritium by mixing with 1−2 mL of Starscint and subsequent scintillation counting.

For the biodistribution studies, rats were euthanized after 72 h for $SPN\text{-}MTX_{cleavable}$ and $Lys\text{-}MTX_{cleavable}$, and at 120 h for $SPN\text{-}MTX_{cleavable}(OtBu)$, $Lys\text{-}MTX_{cleavable}(OtBu)$ and $SPN\text{-}MTX_{stable}$ by intravenous infusion of 1 mL of sodium pentobarbitone (Lethabarb, 320 mg of pentobarbitone sodium/mL) immediately following collection of the final blood sample. Data for $MTX_{stable}(OtBu)$ was reported previously[19] and is reproduced here for comparison. Major organs (liver, kidneys, spleen, pancreas, heart, lungs, brain) were removed, weighed and homogenized in 5−10 mL of Milli-Q water using a Waring miniblender (Extech Equipment Pty. Ltd., Boronia, Australia) for 5 × 10 s intervals. The homogenates were processed and ^{3}H-content was determined as described previously.[27]

Antitumor Efficacy of $Lys\text{-}MTX_{cleavable}(OtBu)$ and $Lys\text{-}MTX_{cleavable}$. Cultured HT1080 cells were isolated by trypsin digestion, washed once in HBSS and then resuspended to 3×10^7 cells/mL in 1:1 Matrigel:PBS on ice. Mice (9−15 per group) were then injected with 100 μL of cells into the left flank with a 25G needle. Tumors were allowed to grow to ~100 mm^3 (approximately 1 week) before treatment began. Mice were injected with MTX, $Lys\text{-}MTX_{cleavable}(OtBu)$ or $Lys\text{-}MTX_{cleavable}$ at 30 mg/kg MTX equivalents or PBS vehicle in a volume of 150 μL via the tail vein once per week for 2 weeks. Body weight and tumor size were measured every 2 days. At the end of the 2 week dosing period, mice were killed by cervical dislocation and blood was collected into heparinized pediatric blood tubes for analysis of markers of hematopoietic or liver toxicity (white cell count, asparate aminotransferase (AST), gamma-glutamyl transferase (GGT); Gribbles Pathological Services, VIC, Australia).

Chromatographic Methods. *HPLC Systems.* Isocratic assays were conducted using a Waters 590 pump, Waters 717 autoinjector and a Waters 486 UV detector (Waters Corporation, Milford, MA, USA) whereas gradient elution was accomplished using a Shimadzu LC-20AD pump and SPD-20A UV detector (NSW, Australia). Assay validation data for all assays are given in the Supporting Information.

MTX-PVG and OtBu-MTX-PVG in Buffered Reaction Solutions. MTX-PVG and OtBu-MTX-PVG were assayed in buffer solutions to determine the stability of the dendrimer constructs in buffer and to probe the extent of release of MTX-PVG and OtBu-MTX-PVG from the dendrimers in the presence of MMPs. MTX-PVG and OtBu-MTX-PVG were separated on a Symmetry Shield RP18 column (4.6 × 100 mm, 3.5 μm particle size, Waters Corporation, Milford, MA, USA) and quantified via UV detection with absorbance set to 307 nm. MTX-PVG was assayed via isocratic elution at a flow rate of 1.5 mL/min using a mobile phase consisting of 14% v/v acetonitrile in 50 mM phosphate

buffer (pH 4.5). A gradient elution method was used to assay OtBu-MTX-PVG and utilized 14% v/v acetonitrile in 50 mM phosphate buffer (pH 4.5) as mobile phase A (MPA) and 50% v/v acetonitrile:water as mobile phase B (MPB). The assay was initiated at 100% v/v MPA and held for 5 min, then linearly changed to 100% v/v MPB over 2 min. The gradient was at 100% MPB for 2 min, returned to 100% MPA over a further 1 min and was subsequently held at 100% mobile phase A for a further 5 min. For MTX-PVG and OtBu-MTX-PVG, 90 μL of reaction solution was injected directly onto the HPLC and quantified relative to a standard curve of MTX-PVG and OtBu-MTX-PVG in the reaction buffer solution containing EDTA.

MTX-PVG and OtBu-MTX-PVG in Cell Culture Medium. To quantify the extent of liberation of MTX-PVG and OtBu-MTX-PVG from cleavable dendrimers in cell culture medium (in the absence of cells) and in culture media containing cells, medium samples (1 mL) were initially spiked with 10 nmol of internal standard (50 μL of a 200 μM solution of MTX in water). MTX was used as the internal standard since preliminary experiments showed that MTX was not liberated from the dendrimer in medium. Proteins in the culture medium were precipitated by addition of an equivalent volume of acetonitrile followed by centrifugation at 3500*g* for 5 min at 4 °C. The supernatant was removed and dried under a stream of nitrogen at 60 °C for 1.5 h and then reconstituted in 200 μL of mobile phase A (5% v/v acetonitrile:95% v/v Milli-Q water/0.2% v/v trifluoroacetic acid, pH 4.5). MTX-PVG, OtBu-MTX-PVG and IS (in a 100 μL injection volume) were separated by HPLC using a Symmetry Shield RP18 column (as above) and linear gradient elution over 15 min. Mobile phase B was 95% v/v acetonitrile:5% v/v Milli-Q water/0.2% v/v trifluoroacetic acid, pH 4.5. The mobile phase gradient sequence was initiated at 100% MPA, linearly decreased over 7 min to 80% MPA, and then further linearly decreased over 4 min to 20% MPA. The system was returned to 100% MPA over 30 s and then held at MPA for 3.5 min. The flow rate was 1.5 mL/min. MTX-PVG, OtBu-MTX-PVG and IS were detected by UV absorbance at 307 nm. MTX-PVG and OtBu-MTX-PVG were quantified relative to a spiked standard curve of MTX-PVG and OtBu-MTX-PVG prepared in blank cell culture medium and processed as above.

MTX-PVG and OtBu-MTX-PVG in Plasma. Plasma samples (0.5 mL) were precipitated by addition of an equivalent volume of acetonitrile and centrifuged at 3500*g* for 5 min at 4 °C. The supernatant was removed and dried under a stream of nitrogen at 60 °C for 1.5 h and then reconstituted in 10% v/v acetonitrile in 50 mM phosphate buffer (pH 4.5). MTX-PVG and OtBu-MTX-PVG (in a 100 μL injection volume) liberated from Lys-$MTX_{cleavable}$, Lys-$MTX_{cleavable}$(OtBu) and SPN-$MTX_{cleavable}$-(OtBu) were separated by HPLC using a Symmetry Shield RP18 column (as above) and linear gradient elution over 15 min. The assay procedure was as described above for MTX-PVG and OtBu-MTX-PVG in cell culture medium except that MPA consisted of 10% v/v acetonitrile in 50 mM phosphate buffer (pH 4.5). The HPLC assay for MTX-PVG liberated from SPN-$MTX_{cleavable}$ utilized a Symmetry Shield RP18 column (as above) and isocratic elution over 15 min in 10% v/v acetonitrile in 50 mM phosphate buffer (pH 4.5).

Size Exclusion Chromatography for Dendrimer in Plasma. Size exclusion chromatography was used to identify the radiolabeled species present in t_0 and 24 h plasma samples and in incubations of dendrimer in fresh plasma (100 μg of dendrimer in 1 mL of plasma at 37 °C for 1 h). Where tritium counts were sufficiently high, sample aliquots were mixed 1:1 with mobile phase before injection onto the column in a final volume of 100−200 μL. Radiolabeled components were separated on a Superdex 200 column (Amersham Biosciences, Piscataway, NJ, USA) with a mobile phase consisting of 50 mM PBS and 0.3 M NaCl (pH 3.5) at a flow rate of 0.5 mL/min as previously described[19] using a Waters 590 pump and Waters 717 autoinjector. Fractions eluting from the column were collected at 1 min intervals (0.5 mL) using a Gilson FC10 fraction collector (John Morris Scientific Pty. Ltd.), mixed with 1.5 mL of Starscint and scintillation counted as described above.

Calculation of Pharmacokinetic Parameters. The amount of radiolabel in each plasma sample was converted to ng dendrimer equivalents using the specific activity of the ^{3}H-labeled dendrimer. Plasma concentrations have been expressed as ng equivalents/mL, realizing that this approach assumes that the ^{3}H-content is still associated with intact dendrimer.

The terminal elimination rate constants (k) were obtained by regression analysis of the individual postdistributive plasma concentration vs time profiles. Half-lives ($t_{1/2}$) were determined from ln 2/k. The area under the plasma concentration vs time profiles ($AUC^{0-\infty}$) were calculated using the linear trapezoidal method. The extrapolated area ($AUC^{tlast-\infty}$) was determined by division of the last measurable plasma concentration (C_{last}) by k. The initial distribution volume (V_c) was calculated by dividing the administered dose by the concentration in plasma at $t = 0$ (C_p^0). Postdistributive volumes of distribution ($V_{D\beta}$) were determined by dividing the administered dose by $k \times AUC^{0-\infty}$. Plasma clearance (Cl) was calculated by dose/$AUC^{0-\infty}$.

Statistics. Organ biodistribution data within the SPN and Lys dendrimer groups were compared by 1-way ANOVA followed by Tukey's test for significant differences. Comparison of pharmacokinetic parameters and organ biodistribution data between comparable SPN and all-lysine dendrimers, and between SPN MTX_{stable} dendrimers and the equivalent SPN $MTX_{cleavable}$ dendrimers, were compared via an unpaired t test. Differences in the extent of MTX-PVG and OtBu-MTX-PVG liberated from $MTX_{cleavable}$ dendrimers at each time point and in the presence of MMP2 and 9 were compared using an unpaired t test. Changes in tumor size in mice administered PBS, MTX, Lys-$MTX_{cleavable}$-(OtBu) or Lys-$MTX_{cleavable}$ were compared by 2-way ANOVA followed by Bonferroni's test for significant differences at each time point. Statistical significance was identified at a level of $p < 0.05$.

RESULTS

Liberation of MTX-PVG from Uncapped or OtBu Capped SPN-$MTX_{cleavable}$ and Lys-$MTX_{cleavable}$ Dendrimers. MMP-catalyzed cleavage of MTX from macromolecular constructs such as dextran-GILGVP-MTX has previously been shown to liberate MTX-PVG.[26] This was confirmed in the current studies by the identification by HPLC of one product in the cleavage experiment that coeluted with authentic MTX-PVG. In the absence of MMP, neither MTX-PVG nor OtBu-MTX-PVG was liberated from the dendrimers in cell culture medium or buffer for up to 3 days. In plasma, less than 2% of MTX-PVG or OtBu-MTX-PVG was liberated from the uncapped and OtBu capped dendrimers respectively, over 3 days.

In the presence of 5 nM MMP2 or MMP9, however, MTX-PVG and OtBu-MTX-PVG liberation was evident from both SPN and Lys based dendrimers. Approximately 5−6% of attached

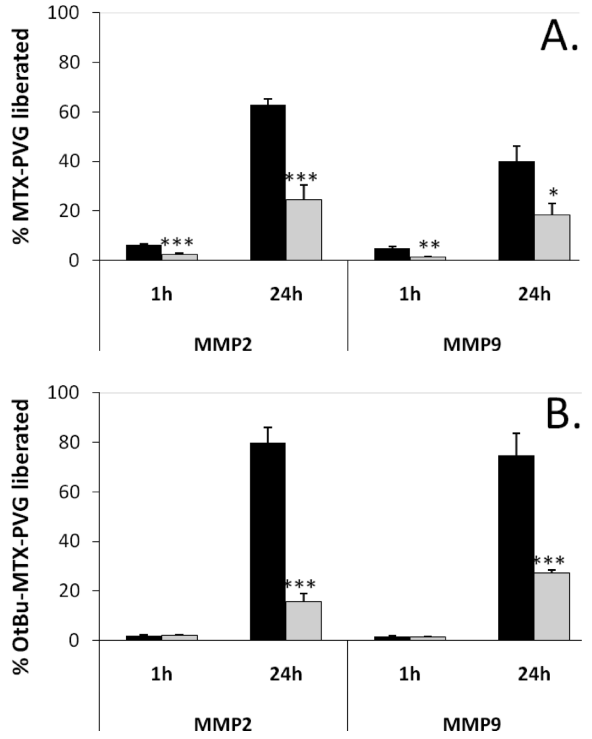

Figure 2. Cleavage of MTX-PVG (panel A) or OtBu-MTX-PVG (panel B) from 5 μM $MTX_{cleavable}$ (panel A) or $MTX_{cleavable}$(OtBu) (panel B) dendrimers in the presence of 5 nM MMP 2 or 9. Black bars represent MTX-PVG or OtBu-MTX-PVG liberated from SPN dendrimers and gray bars represent MTX-PVG or OtBu-MTX-PVG liberated from Lys dendrimers. Values represent mean ± SD ($n = 3$). * represents $p < 0.05$, ** $p < 0.01$, and *** $p < 0.001$ cf. SPN dendrimer.

MTX-PVG was liberated from 5 μM SPN-$MTX_{cleavable}$ in 1 h, and this increased to 38% and 60% at 24 h for MMP9 and MMP2 respectively (Figure 2A). In contrast, liberation of MTX-PVG from Lys-$MTX_{cleavable}$ was more hindered and only 1−3% of MTX-PVG was liberated in 1 h, increasing to 20 and 26% after 24 h in the presence of MMP9 and 2 respectively (Figure 2A). Release of OtBu-MTX-PVG was relatively low from both OtBu capped constructs (SPN-$MTX_{cleavable}$(OtBu) and Lys-$MTX_{cleavable}$-(OtBu)) up to 1 h, but increased significantly over 24 h (Figure 2B) to levels similar to that observed from the uncapped dendrimers (Figure 2A). The liberation of OtBu-MTX-PVG from the SPN-$MTX_{cleavable}$(OtBu) was again significantly greater than that from Lys-$MTX_{cleavable}$(OtBu).

The proportion of MTX-PVG or OtBu-MTX-PVG released from SPN-$MTX_{cleavable}$ and Lys-$MTX_{cleavable}$ dendrimers was also examined under conditions reflective of those encountered in the cell culture cytotoxicity studies. HT1080 cells were exposed to 32 μM MTX equivalents (or 14.4 μg MTX equivalents) of dendrimer (the concentration of dendrimer required to inhibited cell replication by approximately 75%) for 2 days and the liberation of MTX-PVG or OtBu-MTX-PVG measured by HPLC. Under these conditions, 0.11 ± 0.01 μg and 0.33 ± 0.02 μg MTX equivalents of MTX-PVG were liberated from SPN-$MTX_{cleavable}$ and Lys-$MTX_{cleavable}$ respectively and 0.40 ± 0.05 μg and 0.89 ± 0.07 μg MTX equivalents of OtBu-MTX-PVG were liberated from SPN-$MTX_{cleavable}$(OtBu) and Lys-$MTX_{cleavable}$(OtBu) respectively.

Release of MTX-PVG or OtBu-MTX-PVG from the Lys-$MTX_{cleavable}$ construct was therefore relatively more efficient under cell culture conditions, when compared with in vitro release in the simple enzyme preparations where release from the SPN-$MTX_{cleavable}$ construct was favored.

In Vitro Cytotoxicity of Uncapped or OtBu Capped SPN-$MTX_{cleavable}$ and Lys-$MTX_{cleavable}$ Dendrimers. Free MTX reduced cell viability of HT1080 cells over 2 days with an IC_{50} of approximately 0.2 μM. MTX-PVG was approximately 10-fold less active against HT1080 cells than free MTX as reported previously by Chau[26] (Figure 3A). OtBu-MTX-PVG was a further 10-fold less cytotoxic than MTX-PVG against HT1080 cells consistent with previous data showing that protection of the α-carboxyl group of MTX results in reduced in vitro activity[29] (Figure 3A).

Interestingly, however, for both SPN and Lys dendrimers, there was little difference in the cytotoxicity of the cleavable constructs against HT1080 cells, regardless of the presence or absence of the OtBu capping group (IC_{50} values were approximately 20−40 μM and 2−4 μM MTX equivalents for SPN and Lys dendrimers respectively, Figure 3B and Figure 3C). The stable construct SPN-MTX_{stable} showed very poor in vitro cytotoxicity (IC_{50} approximately 500 μM), suggesting that the loss of cell viability mediated by the presence of the OtBu capped or uncapped dendrimers was due to the liberation of MTX-PVG or OtBu-MTX-PVG rather than toxicity due to intact dendrimer. OtBu-MTX-PVG and MTX-PVG were well separated by HPLC, and no evidence of loss of the OtBu capping group from OtBu-MTX-PVG was evident in these in vitro studies. Nonetheless the capping group (*t*-butanol) also showed no indication of cytotoxicity in the current assay up to 500 μM.

Intravenous Pharmacokinetics and Biodistribution of MTX-Conjugated Dendrimers. SPN-MTX_{stable}(OtBu) was previously shown to be cleared slowly from plasma after intravenous administration with a terminal half-life of approximately 2 days.[18] In contrast, following intravenous administration of the uncapped cleavable construct (SPN-$MTX_{cleavable}$), the dendrimer was rapidly cleared (~10-fold increase in Cl, Table 3). After 3 days, approximately 50% of the injected radiolabel was identified in liver and spleen, with little of the injected radiolabel identified in other organs collected (Figure 4A,B, Table 3). Notably, reprotection of the α-carboxyl of MTX on the cleavable dendrimer significantly slowed plasma clearance and increased terminal half-life to values similar to those observed for the OtBu-capped stably conjugated system. It was also apparent that removal of the capping group in the stable construct, i.e. SPN-MTX_{stable}, also decreased terminal half-life (to approximately 20 h) and increased uptake into the liver when compared to SPN-MTX_{stable}(OtBu), although the difference was not as significant as that observed for the uncapped cleavable construct. The data therefore suggest that removal of the capping group and incorporation of the cleavable linker increased clearance, reduced volume of distribution and reduced half-life and that this occurred in a highly synergistic fashion for the uncapped and cleavable construct.

The data obtained for the all-lysine dendrimers showed a similar trend to the SPN dendrimers (Figure 4C,D, Table 3), although the uncapped Lys-$MTX_{cleavable}$ dendrimer was cleared approximately twice as rapidly from plasma than the equivalent SPN dendrimer (SPN-$MTX_{cleavable}$). The extent of elimination of injected radiolabel via the urine did not differ significantly between SPN and Lys dendrimers, although a trend toward higher urinary excretion of radiolabel was evident with the Lys construct (Table 3). The proportion of injected ^3H excreted in each collection period is reported in the Supporting Information.

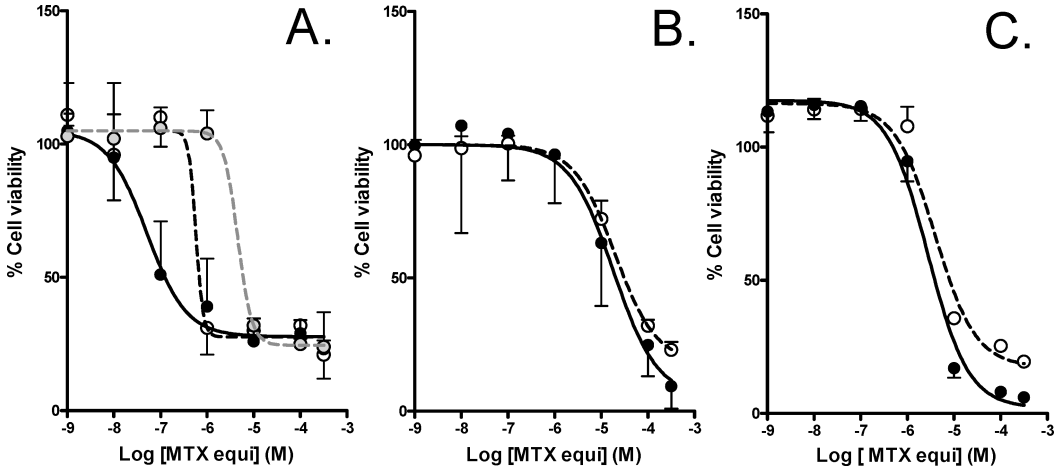

Figure 3. Cytotoxicity of MTX constructs against HT1080 cells over a 48 h incubation period determined by MTT assay. Panel A: free MTX (closed symbols and solid black line), MTX-PVG (open symbols and broken black line), OtBu-MTX-PVG (gray symbols and broken gray line). Panel B: SPN-$MTX_{cleavable}$ (closed symbols and solid black line), SPN-$MTX_{cleavable}$(OtBu) (open symbols and broken black line). Panel C: Lys-$MTX_{cleavable}$ (closed symbols and solid black line), Lys-$MTX_{cleavable}$(OtBu) (open symbols and broken black line). Lines represent best fit curves calculated via a variable slope sigmoidal fitting program (where $Y = 100/(1 + 10^{[\mathrm{LogIC50}-X](\mathrm{Hill\ slope})})$) in GraphPad Prism. Values are represented as mean ± SD ($n = 3$).

Table 3. Pharmacokinetic Parameters for G5 MTX Conjugated Dendrimers[a]

	SPN MTX_{stable}		SPN $MTX_{cleavable}$		Lys $MTX_{cleavable}$	
	α-OtBu	α-OH	α-OtBu	α-OH	α-OtBu	α-OH
Cl (mL/h)	0.6 ± 0.0*	0.9 ± 0.1	0.7 ± 0.0*	7.2 ± 0.7†	0.5 ± 0.0*	19.6 ± 3.3#
V_c (mL)	16.0 ± 1.1	13.8 ± 1.7	13.9 ± 2.2	14.4 ± 1.3	14.9 ± 1.2	15.7 ± 2.6
$V_{D\beta}$ (mL)	43.1 ± 1.5*	24.9 ± 2.1	27.2 ± 1.3*†	11.6 ± 1.2†	22.6 ± 3.5*	7.6 ± 1.2
$t_{1/2}$ (h)	51.3 ± 3.2*	19.9 ± 0.9	26.4 ± 1.6*†	1.1 ± 0.0†	33.3 ± 3.3*#	0.3 ± 0.1#
% injected ^{3}H in urine	1.2 ± 0.1	1.2 ± 0.2	9.0 ± 3.2*†	1.9 ± 0.1†	13.6 ± 1.5*#	2.1 ± 1.0
% injected ^{3}H in liver	12.1 ± 2.0*	17.0 ± 2.0	7.6 ± 3.0*	51.7 ± 9.6†	10.2 ± 1.0*	85.4 ± 0.2#

[a] Values are represented as mean ± SD ($n = 3$). Statistical differences ($p < 0.05$) between OtBu capped and uncapped (OH) dendrimers are represented by * (noted on the OtBu capped dendrimer), differences between equivalent SPN and Lys cleavable dendrimers are represented by # (noted on the Lys dendrimer), and significant differences between SPN-MTX_{stable}(OtBu) and the equivalent SPN-$MTX_{cleavable}$ dendrimer or between SPN-MTX_{stable}-(OH) and the equivalent SPN-$MTX_{cleavable}$ dendrimer are represented by † (significance is indicated on the SPN-$MTX_{cleavable}$ dendrimers only). The results for SPN-MTX_{stable}(OtBu) are reproduced from Kaminskas et al.[18].

Examination of Radiolabeled Species Present in Plasma from Rats Administered MTX-Conjugated Dendrimers. In an attempt to explain the differences in plasma clearance and hepatic targeting of the stable vs cleavable and capped vs uncapped MTX-conjugated dendrimers, the radiolabeled species present in plasma were investigated by size exclusion chromatography. The profiles shown in Figure 5 for SPN-MTX_{stable} and profiles reported previously for SPN-MTX_{stable}(OtBu)[18] suggest that the stable constructs exist in plasma primarily as intact dendrimer. The dendrimers containing a cleavable PVGLIG linker also existed as single species in buffer (Figure 5). However, the dendrimers containing the cleavable linker formed high molecular weight species in the presence of plasma that eluted several minutes before the intact dendrimer. The proportional contribution of the high MW product to the t_0 and 24 h plasma samples was more evident for the capped cleavable dendrimer (SPN-$MTX_{cleavable}$(OtBu) and Lys-$MTX_{cleavable}$(OtBu)) than for dendrimers devoid of OtBu protection. No clear differences were evident in the SEC profiles of dendrimers containing an SPN outer generation when compared with dendrimers composed of all-lysine.

Antitumor Activity of OtBu Capped and Uncapped Lys-$MTX_{cleavable}$ Dendrimers against HT1080 Tumors in a Mouse Xenograft Model. Intravenous administration of free MTX (30 mg/kg) weekly for 2 weeks resulted in a significant reduction in the growth of HT1080 tumors, such that on day 12 mice receiving weekly MTX showed a 37% reduction in tumor size when compared to mice that received vehicle (PBS) alone (Figure 6A). Mice receiving weekly dosing of Lys-$MTX_{cleavable}$-(OtBu) at 30 mg/kg MTX equivalents also showed a significant (63%) reduction in tumor size on day 12 when compared to mice receiving vehicle, although this difference was not statistically significant compared to data obtained in mice administered equimolar quantities of MTX. In contrast, however, mice receiving weekly dosing of the uncapped Lys-$MTX_{cleavable}$ construct at 30 mg/kg MTX equivalents showed no evidence of a reduction of tumor growth when compared to control mice that received vehicle alone (PBS, Figure 6B). The study was terminated at 12 days in all groups on ethical grounds as tumor progression resulted in signs of toxicity (body weight decreased to the maximum allowable loss, Supporting Information). Markers of systemic toxicity, including white blood cell count and plasma levels of

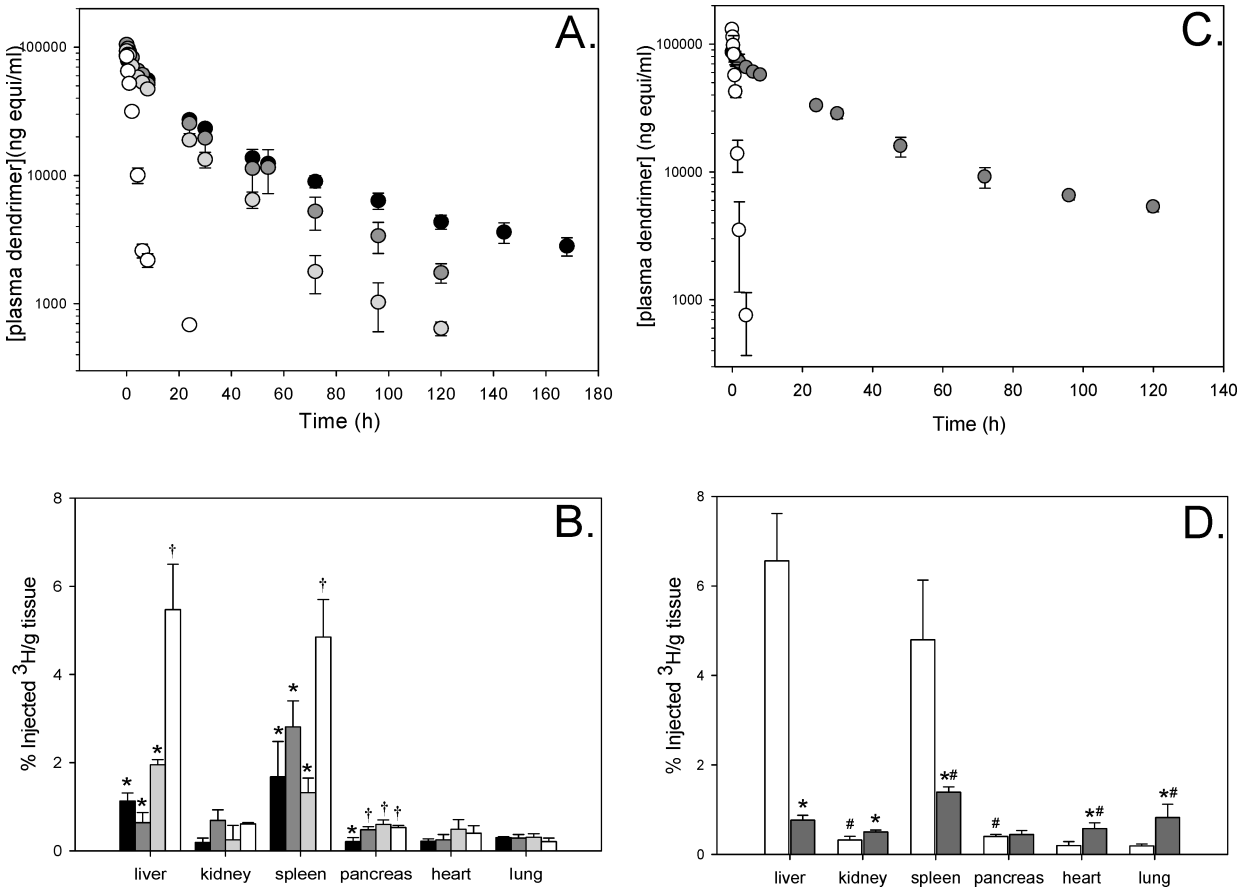

Figure 4. Plasma concentration−time profiles and biodistribution of MTX-conjugated dendrimers after a single 5 mg/kg iv administration to SD rats. Panels represent plasma concentration−time profiles (panel A) and organ biodistribution (panel B) of SPN dendrimers and plasma concentration−time profiles (panel C) and organ biodistribution (panel D) of Lys dendrimers alone. Symbols represent SPN-MTX_{stable}(OtBu) (closed symbols), SPN- and Lys-$MTX_{cleavable}$(OtBu) (dark gray symbols), SPN-MTX_{stable} (light gray symbols), SPN- and Lys-$MTX_{cleavable}$ (open symbols). Values are represented as mean ± SD (n = 3). * represents $p < 0.05$ cf. $MTX_{cleavable}$ uncapped dendrimers, # represents $p < 0.05$ cf. equivalent SPN dendrimer, † represents $p < 0.05$ cf. MTX_{stable}(OtBu). Data for SPN-MTX_{stable}(OtBu) is reproduced from Kaminskas et al.[18]

liver enzymes, revealed no significant differences between mice in the 4 groups (see Supporting Information).

DISCUSSION

Several previous studies have described the construction of PEG dendrimers which exhibit properties consistent with utility in cancer chemotherapy such as a long plasma half-life and the capacity to preferentially accumulate in solid tumors.[17,18,30,31] In this laboratory we have previously examined the pharmacokinetic properties of either fully PEGylated poly-L-lysine dendrimer constructs[28] or PEG dendrimers conjugated with MTX.[18] In our previous studies with PEGylated, MTX-conjugated dendrimers the α-carboxyl group of MTX was intentionally capped with OtBu to prevent the potential complicating effects of MTX interaction with folate receptors on interpretation of the pharmacokinetic profiles.[18] Model dendritic systems were also employed where MTX was conjugated to the dendrimer via a physiologically stable (amide) linker, again in order to preclude the complicating effects of drug liberation and subsequent biodegradation of the construct on the pharmacokinetic profile. In the current study, the initial aim was therefore to examine the pharmacokinetics of PEGylated dendritic complexes where MTX was conjugated to the dendrimer via an MMP cleavable hexapeptide linker (PVGLIG) in order to provide for specificity in drug release at the tumor site, and where the OtBu capping group was removed (since previous studies have suggested that the α-carboxyl group of MTX is critical to activity[29,32]). Surprisingly, however, the data reported here reveal that the uncapped dendrimers are cleared from plasma very rapidly, raising questions as to their suitability for EPR in solid tumors. The current studies were therefore expanded to examine whether capping the free carboxyl group of MTX conjugated dendrimers might be utilized to enhance in vivo utility.

The PVGLIG linker examined here was stable over several days in cell culture medium, plasma and buffer. When exposed to either MMPs in buffer or cancer cells that overexpress MMPs, however, release of OtBu-MTX-PVG or MTX-PVG was evident from the uncapped or OtBu capped dendrimers respectively. The PVGLIG linker has previously been reported to be more labile in the presence of MMP2 than MMP9;[26] however, this was only evident in the current studies with the uncapped dendrimers (Figure 2A), and the OtBu protected dendrimers appeared to be equally susceptible to cleavage by MMP2 and MMP9 (Figure 2B). Interestingly, MTX-PVG or OtBu-MTX-PVG liberation was more effective from the SPN dendrimer when compared to the Lys dendrimers in the presence of purified MMPs, suggesting a conformational difference resulting in greater availability of the hexapeptide to enzymatic attack in the symmetrical SPN construct

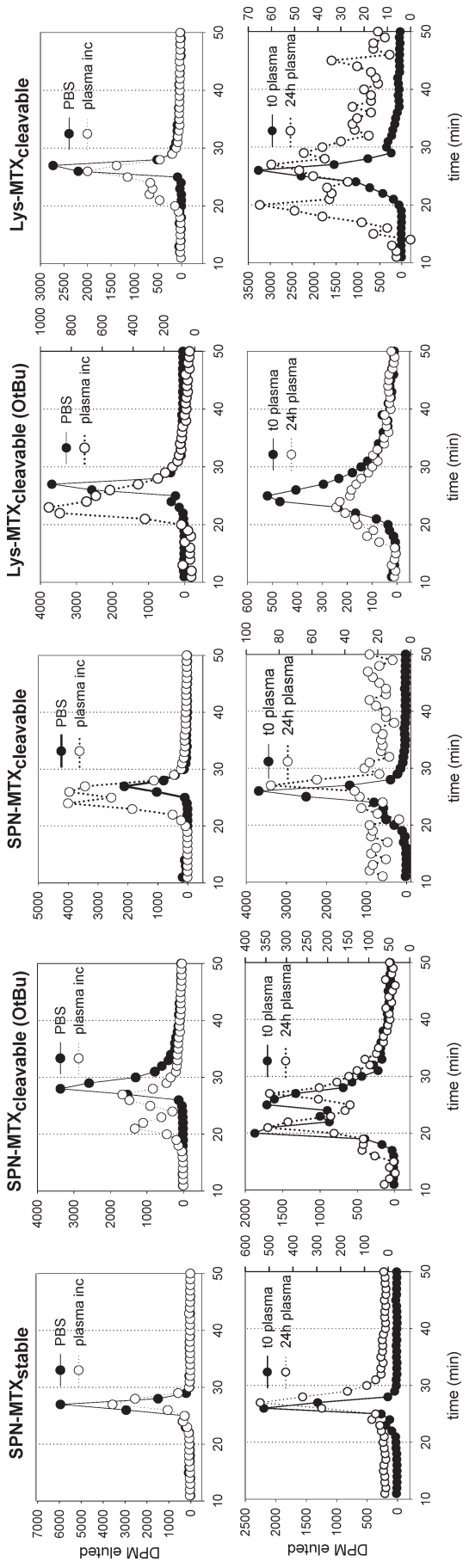

Figure 5. Size exclusion chromatography profiles of MTX-conjugated dendrimers after in vitro incubation in PBS and plasma (top panel) and in t_0 and t_{24h} plasma samples taken from rats administered 5 mg/kg dendrimer intravenously (bottom panel). ^{3}H-Labeled species were separated on a Superdex 200 column.

when compared to the asymmetrical Lys construct. In cell culture, however, the release of MTX-PVG or OtBu-MTX-PVG was approximately 2−3-fold greater from the Lys dendrimers when compared to the SPN dendrimers, possibly reflecting a greater propensity toward biodegradation of the Lys dendrimer (and therefore increased enzymatic access to the hexapeptide) when compared to the SPN variant.

Removal of the OtBu capping group had a profound impact on the pharmacokinetics of the dendrimer (Figure 4) leading to a significant increase in clearance (Cl), decrease in volume of distribution (V_D) and therefore decrease in terminal half-life, for both Lys and SPN dendrimers. This was accompanied by an increase in uptake into the liver and a reduction in renal clearance. The increase in clearance was most notable in systems containing the hexapeptide linker. For example, removal of the OtBu capping group from the SPN-MTX$_{stable}$ dendrimer resulted in no significant change to clearance, a small decrease in V_D (2-fold) and therefore a moderate (2-fold) change to half-life. In contrast, where MTX was conjugated to the dendrimer via the hexapeptide linker, removal of the capping group led to a profound (10-fold) increase in clearance, a significant increase in liver uptake and a 20-fold reduction in half-life. This was not a product of the liberation of MTX-PVG from the dendrimer since a similar Lys-MTX dendrimer constructed using a scrambled (non-MMP labile) GIVGPL peptide linker showed similarly rapid plasma clearance and uptake via the liver (see Supporting Information). Comparison of the plasma pharmacokinetics and organ deposition patterns of the SPN vs Lys dendrimers revealed little differences in in vivo profiles suggesting that the nature of the outer Lys or SPN layer had limited impact on disposition, and that the presence or absence of the hexapeptide linker and/or OtBu capping group dominated clearance patterns.

Together, the data suggest that revealing the α-carboxyl group of MTX resulted in dendrimer recognition by the liver and that this was most effective when the MTX was projected further from the core of the dendrimer by inclusion of the relatively high molecular weight hexapeptide linker (Figure 7). Studies are ongoing to evaluate the mechanism of liver uptake of these systems. To our knowledge this is the first report of very rapid, highly significant liver uptake of uncapped MTX-conjugated nanostructures and may have significant ramifications for the design of other MTX-conjugated nanomedicines where the relative dimensions of the PEG layer and MTX linker are similar to those examined here.

Previous studies with other anionic dendrimers (aryl sulfonate derived systems) have also demonstrated that the presence of anionic surface functionalities may result in increased liver uptake. In the case of the aryl sulfonates, however, this occurred in parallel with an increase in opsonization.[33] In contrast, here, the degree of opsonization (as evidenced by the appearance of a high molecular weight species after exposure of the dendrimer to plasma) was not related to the presence of uncapped MTX (i.e., the anionic group), or to the presence of the hexapeptide linker or indeed liver uptake. Rather, the patterns of clearance of the dendrimers that formed high molecular weight constructs were variable. For example, after administration of all the hexapeptide containing constructs, a high molecular weight species was evident in plasma, but only those conjugated to uncapped MTX were rapidly taken up into the liver. It appears, therefore, that the dominant feature in dictating rapid clearance was the presence of the uncapped MTX moiety in combination with the

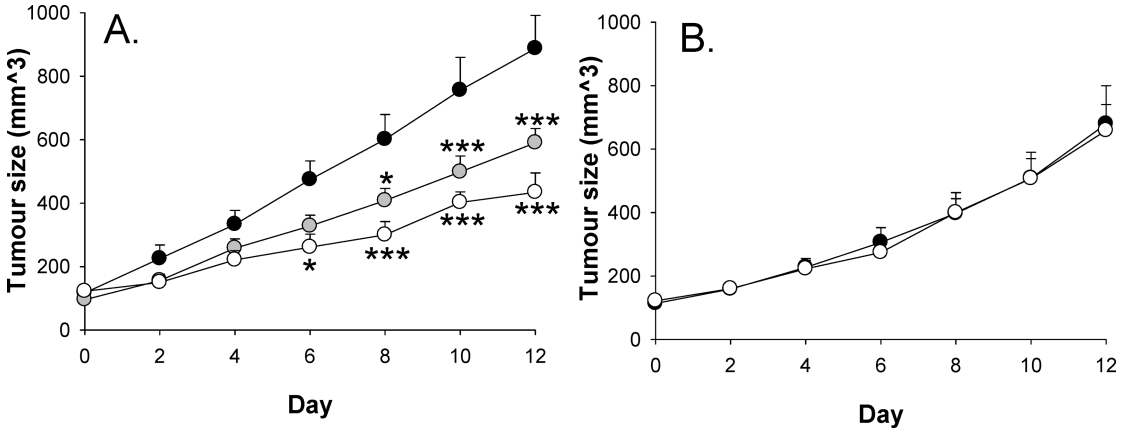

Figure 6. Antitumor efficacy of MTX (gray symbols) and MTX dendrimers (open symbols) against HT1080 tumors in female *nu/nu* mice. PBS treated control mice are represented by closed symbols. Panel A: Antitumor efficacy of Lys-$MTX_{cleavable}$(OtBu). Panel B: Antitumor efficacy of Lys-$MTX_{cleavable}$. Mice were administered 30 mg/kg MTX equivalents of free MTX or dendrimer on day 0 and day 7, and tumor volume was measured with a pair of calipers every 2 days. Values represent mean ± SEM (n = 9−15). * represents $p < 0.05$ and *** represents $p < 0.001$ cf. PBS control mice.

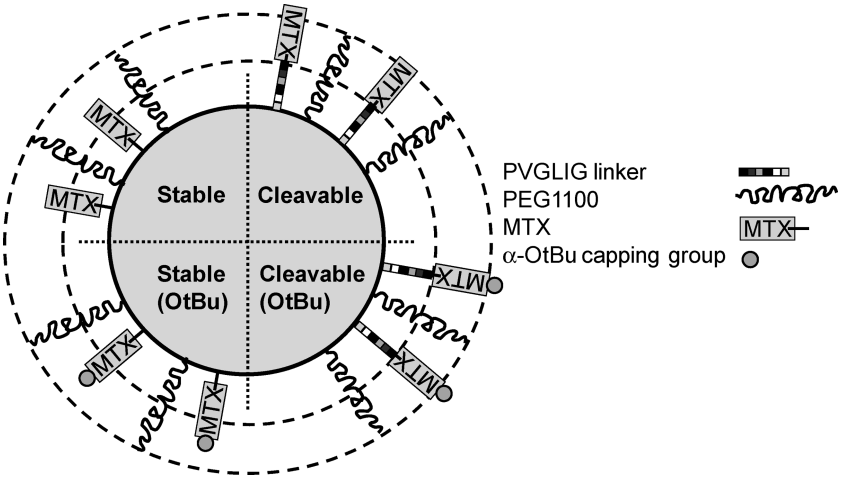

Figure 7. Schematic representation of the dendrimers utilized in the current study showing PEG and methotrexate (±OtBu capping group) linked to the dendrimer surface via either a stable amide linker or the MMP cleavable PVGLIG linker.

high molecular weight linker rather than the presence or absence of opsonization.

The molecular weight of the PVGLIG linker (~640 Da) was approximately half of that of the surface PEG groups (1100 Da), and MTX was of a similar size (~450 Da) to the linker. It is therefore possible that the insertion of the hexapeptide linker resulted in projection of MTX to the biological interface of the PEGylated dendrimer thereby more effectively presenting the free carboxyl group on the uncapped MTX to RES organs including the liver. In turn this might be expected to lead to more effective recognition of the polyanionic surface of the uncapped MTX-conjugated dendrimer and subsequent uptake by resident phagocytic cells (Figure 7).[33] In contrast, in the absence of the hexapeptide linker the MTX molecule may have remained relatively obscured from biological interaction by the adjacent 1100 Da PEG chains.

It is also possible that targeting of the $MTX_{cleavable}$ dendrimers to the RES organs was due to recognition by the reduced folate carrier since the liver has been shown (at least in humans) to contain a high level of reduced folate carrier mRNA (consistent with the need for high levels of the carrier in order to facilitate hepatic storage of excess plasma folate[34]). However, the kidneys, lungs and parts of the brain also express high levels of reduced folate carrier mRNA,[34] but did not show increased accumulation of dendrimer. Instead, dendrimer was distributed almost equally to the liver and spleen. Data on the presence of the reduced folate carrier in the liver and spleen of rats is not available, although in mouse liver, the reduced folate carrier is expressed on the plasma membrane of hepatocytes and not in other stromal cells, while in the spleen, it is expressed only on the plasma membrane of cells in the red pulp.[35] The folate receptor was not expected to be involved in the liver targeting of the $MTX_{cleavable}$ dendrimers since in humans and rats the liver does not express high levels of this receptor or its transcript.[36] Furthermore, cellular uptake of antifolates into cancer cells has been demonstrated to occur preferentially via the reduced folate carrier, even when the folate receptor is expressed to very high levels.[37]

The pharmacokinetic data therefore suggest that uncapped methotrexate systems are recognized by RES clearance mechanism that may involve either nonspecific uptake (possibly via an electrostatic interaction with the anionic charge on the dendrimer) or uptake by the reduced folate carrier, and are rapidly

removed from the circulation. This significantly limits the potential utility of dendritic targeting systems that rely on long systemic circulation.

In light of the reduced plasma circulation times of the uncapped MTX dendrimers, the potential utility of the capped dendrimers as improved delivery systems was subsequently examined. Initial in vitro cytotoxicity investigations revealed that dendrimers comprising capped MTX conjugated to the dendrimer surface via the cleavable PVGLIG linker retained in vitro cytotoxic activity against HT1080 cells, although the dendrimer was approximately 10- and 100-fold less active than molar equivalent concentrations of MTX-PVG and free MTX. Interestingly, the capped MTX dendrimers were similarly cytotoxic to equimolar concentrations of OtBu-MTX-PVG. The reduced in vitro cytotoxicity of the OtBu capped dendrimers is consistent with the results of others who have reported that capping the α-carboxyl group on MTX reduces cytotoxic activity of the drug in vitro[29] and that drug conjugated systems show significantly reduced in vitro cytotoxic activity when compared to free drug.[26] Of particular significance to the current studies, however, was the realization that capping the α-carboxyl group on MTX did not change the in vitro activity of the MTX-dendrimers (SPN-$MTX_{cleavable}$(OtBu) and Lys-$MTX_{cleavable}$(OtBu)) when compared to the equivalent uncapped constructs (SPN-$MTX_{cleavable}$ and Lys-$MTX_{cleavable}$) (Figure 3B,C). This was surprising given the reduced cytotoxic activity of OtBu-MTX-PVG when compared to MTX-PVG, and may suggest alternate modes of cytotoxicity rather than simple extracellular liberation of OtBu-MTX-PVG or MTX-PVG. For example, cellular uptake of intact dendrimer may lead to differential rates of liberation of OtBu-MTX-PVG or MTX-PVG and/or the prospect of intracellular liberation of the *t*-butyl capping group by cytosolic esterases. Cellular uptake of the OtBu capped constructs via the folate or antifolate receptor pathway, however, is unlikely since others have suggested that the MTX free carboxylate is required to provide affinity.[29] In contrast, nonclassical antifolates (such as trimetrexate), which are less polar than classical antifolates, retain activity but exhibit folate/antifolate receptor independent uptake into cancer cells.[38] It is possible, therefore, that this mechanism of cellular uptake may be utilized by OtBu modified MTX or OtBu modified MTX dendrimers and that capping the carboxylate charge may enhance uptake. Further studies are required to explore the potential for differential modes of cellular entry and cytotoxicity of the capped and uncapped constructs. Critically, however, in vivo activity is a function of pharmacokinetic properties (i.e. the extent of targeting), drug release and potency. Polymer conjugates which exhibit marked EPR may therefore be more active in vivo than free drug, even though their intrinsic potency is lower. That is, improved tumor targeting can overcome the challenges associated with the requirement for conversion to free drug.[10]

Given the in vitro activity of the capped MTX linked constructs and their superior pharmacokinetic properties when compared to the uncapped constructs, the antitumor activity of $MTX_{cleavable}$(OtBu) and $MTX_{cleavable}$ dendrimers was subsequently compared in a mouse xenograft model. Although the in vitro release data suggested faster liberation of MTX-PVG and OtBu-MTX-PVG from the SPN dendrimers in the presence of MMPs, the Lys dendrimers were progressed to the in vivo trials. The Lys dendrimers were utilized since MTX-PVG and OtBu-MTX-PVG release from the Lys dendrimers was higher than that of the SPN dendrimers in cell culture, the Lys dendrimers were more active in cell culture than the SPN dendrimers and the all-lysine systems had greater potential for in vivo degradation of the polylysine scaffold.[18] Previous studies have also shown that the lysine dendrimer cores (that might be expected to be generated by surface liberation of conjugated drug) show reduced accumulation into RES organs when compared to equivalent SPN constructs.[18]

In the xenograft studies, administration of either free MTX or Lys-$MTX_{cleavable}$(OtBu) resulted in significantly slower tumor growth when compared to control mice. Tumors in animals administered Lys-$MTX_{cleavable}$(OtBu) were approximately 20% smaller than those in mice administered an equivalent molar dose of methotrexate, although this difference was not statistically significant, in contrast to the data of Chau et al.,[24] who reported better antitumor activity for a more labile 1:1 dextran-MTX construct. Lys-$MTX_{cleavable}$ showed no activity against HT1080 tumors, presumably as a result of rapid clearance from plasma and uptake into the liver.

In summary, protection of the α-carboxyl group on MTX conjugated dendrimers prevented rapid accumulation of the dendrimer in the liver and allowed for extended circulation times in the systemic circulation (properties consistent with improved EPR) without attenuating in vitro or in vivo cytotoxic efficacy. The data suggest that protecting the α-carboxyl functionality on MTX-conjugated dendrimers (or potentially other nanoparticulate MTX systems) may provide a means of improving biodistribution, tumor targeting and antitumor activity of MTX derived nanomedicines.

■ ASSOCIATED CONTENT

Supporting Information. Additional experimental details. This material is available free of charge via the Internet at http://pubs.acs.org.

■ AUTHOR INFORMATION

Corresponding Author

*C.J.H.P.: Drug Delivery, Disposition and Dynamics, Monash Institute of Pharmaceutical Sciences, Monash University, 381 Royal Parade, Parkville, VIC, Australia, 3052; e-mail, chris.porter@monash.edu; tel, +61 3 9903 9649; fax, +61 3 9903 9583.

■ ACKNOWLEDGMENT

L.M.K. was supported by a NHMRC Australian Biomedical Training Fellowship. This work was funded by an ARC Linkage grant.

■ REFERENCES

(1) Cho, K.; Wang, X.; Nie, S.; Chen, Z. G.; Shin, D. M. Therapeutic nanoparticles for drug delivery in cancer. *Clin. Cancer Res.* **2008**, *14*, 1310–1316.

(2) Saad, M.; Garbuzenko, O. B.; Ber, E.; Chandna, P.; Khandare, J. J.; Pozharov, V. P.; Minko, T. Receptor targeted polymers, dendrimers, liposomes: which nanocarrier is the most efficient for tumor-specific treatment and imaging?. *J. Controlled Release* **2008**, *130*, 107–14.

(3) Thanou, M.; Duncan, R. Polymer-protein and polymer-drug conjugates in cancer therapy. *Curr. Opin. Invest. Drugs* **2003**, *4*, 701–709.

(4) Witte, M. H.; Jones, K.; Wilting, J.; Dictor, M.; Selg, M.; McHale, N.; Gershenwald, J. E.; Jackson, D. G. Structure function relationships in the lymphatic system and implications for cancer biology. *Cancer Metastasis Rev.* **2006**, *25*, 159–184.

(5) Padera, T. P.; Kadambi, A.; di Tomaso, E.; Carreira, C. M.; Brown, E. B.; Boucher, Y.; Choi, N. C.; Mathisen, D.; Wain, J.; Mark, E. J.; Munn, L. L.; Jain, R. K. Lymphatic metastasis in the absence of functional intratumor lymphatics. *Science* **2002**, *296*, 1883–1886.

(6) Pathak, A. P.; Artemov, D.; Ward, B. D.; Jackson, D. G.; Neeman, M.; Bhujwalla, Z. M. Characterizing extravascular fluid transport of macromolecules in the tumor interstitium by magnetic resonance imaging. *Cancer Res.* **2005**, *65*, 1425–1432.

(7) Cattel, L.; Ceruti, M.; Dosio, F. From conventional to stealth liposomes: a new frontier in cancer chemotherapy. *Tumori* **2003**, *89*, 237–249.

(8) Schmitt-Sody, M.; Strieth, S.; Krasnici, S.; Sauer, B.; Schulze, B.; Teifel, M.; Michaelis, U.; Naujoks, K.; Dellian, M. Neovascular targeting therapy: paclitaxel encapsulated in cationic liposomes improves antitumoral efficacy. *Clin. Cancer Res.* **2003**, *9*, 2335–2341.

(9) Agarwal, A.; Gupta, U.; Asthana, A.; Jain, N. K. Dextran conjugated dendritic nanoconstructs as potential vectors for anti-cancer agent. *Biomaterials* **2009**, *30* (21), 3588–3596.

(10) Chau, Y.; Dang, N. M.; Tan, F. E.; Langer, R. Investigation of targeting mechanism of new dextran-peptide-methotrexate conjugates using biodistribution study in matrix-metalloproteinase-overexpressing tumor xenograft model. *J. Pharm. Sci.* **2006**, *95*, 542–551.

(11) Etrych, T.; Chytil, P.; Mrkvan, T.; Sirova, M.; Rihova, B.; Ulbrich, K. Conjugates of doxorubicin with graft HMPA copolymers for passive tumor targeting. *J. Controlled Release* **2008**, *132*, 184–192.

(12) Oyewumi, M. O.; Yokel, R. A.; Jay, M.; Coakley, T.; Mumper, R. J. Comparison of cell uptake, biodistribution and tumor retention of folate-coated and PEG-coated gadolinium nanoparticles in tumor-bearing mice. *J. Controlled Release* **2004**, *95*, 613–626.

(13) Shenoy, D.; Little, S.; Langer, K.; Amiji, M. Poly(ethylene oxide)-modified poly(beta-amino ester) nanoparticles as a pH-sensitive system for tumor-targeted delivery of hydrophobic drugs: part 2. In vivo distribution and tumor localization studies. *Pharm. Res.* **2005**, *22*, 2107–2114.

(14) Khandare, J. J.; Jayant, S.; Singh, A.; Chandna, P.; Wang, Y.; Vorsa, N.; Minko, T. Dendrimer versus linear conjugate: Influence of polymeric architecture on the delivery and anticancer effect of paclitaxel. *Bioconjugate Chem.* **2006**, *17*, 1464–72.

(15) Malik, N.; Evagorou, E. G.; Duncan, R. Dendrimer-platinate: a novel approach to cancer chemotherapy. *Anti-Cancer Drugs* **1999**, *10*, 767–776.

(16) Patri, A. K.; Kukowska-Latallo, J. F.; Baker, J. R., Jr. Targeted drug delivery with dendrimers: comparison of the release kinetics of covalently conjugated drug and non-covalent drug inclusion complex. *Adv. Drug Delivery Rev.* **2005**, *57*, 2203–2214.

(17) Lee, C.; Gillies, E.; Fox, M.; Guillaudeu, S.; Frechet, L.; Dy, E.; Szoka, F. A single dose of doxorubicin-functionalized bow-tie dendrimer cures mice bearing C-26 colon carcinomas. *Proc. Natl. Acad. Sci. U.S.A.* **2006**, *103*, 16679–16654.

(18) Kaminskas, L. M.; Kelly, B.; McLeod, V.; Boyd, B. J.; Krippner, G. Y.; Williams, E. D.; Porter, C. J. H. Pharmacokinetics and tumour disposition of PEGylated methotrexate conjugated poly-L-lysine dendrimers. *Mol. Pharmaceutics* **2009**, *6*, 1190–1204.

(19) Kukowska-Latallo, J. F.; Candido, K. A.; Cao, Z.; Nigavekar, S. S.; Majoros, I. J.; Thomas, T. P.; Balogh, L. P.; Khan, M. K.; Baker, J. R. Nanoparticle targeting of anticancer drug improves therapeutic response in animal model of human epithelial cancer. *Cancer Res.* **2005**, *65*, 5317–5324.

(20) Kono, K.; Kojima, C.; Hayashi, N.; Nishisaka, E.; Kiura, K.; Watarai, S.; Harada, A. Preparation and cytotoxic activity of poly(ethylene glycol)-modified poly(amidoamine) dendrimers bearing adriamycin. *Biomaterials* **2008**, *29*, 1664–75.

(21) Gurdag, S.; Khandare, J.; Stapels, S.; Matherly, L. H.; Kannan, R. M. Activity of dendrimer-methotrexate conjugates on methotrexate-sensitive and -resistant cell lines. *Bioconjugate Chem.* **2006**, *17*, 275–283.

(22) Cheng, Y.; Xu, T. The effect of dendrimers on the pharmacodynamic and pharmacokinetic behaviors of non-covalently or covalently attached drugs. *Eur. J. Med. Chem.* **2008**, *43*, 2291–2297.

(23) Jain, N. K.; Asthana, A. Dendritic systems in drug delivery applications. *Expert Opin. Drug Delivery* **2007**, *4*, 495–512.

(24) Chau, Y.; Padera, R. F.; Dang, N. M.; Langer, R. Antitumour efficacy of a novel polymer-peptide-drug conjugate in human tumour xenograft models. *Int. J. Cancer* **2005**, *118*, 1519–1526.

(25) Aguilera, T. A.; Olson, E. S.; Timmers, M. M.; Jiang, T.; Tsien, R. Y. Systemic in vivo distribution of activatable cell penetrating peptides is superior to that of cell penetrating peptides. *Integr. Biol.* **2009**, *1*, 371–381.

(26) Chau, Y.; Tan, F. E.; Langer, R. Synthesis and characterisation of dextran-peptide-methotrexate conjugates for tumor targeting via mediation by matrix metalloproteinase II and matrix metalloproteinase IX. *Bioconjugate Chem.* **2004**, *15*, 931–941.

(27) Boyd, B. J.; Kaminskas, L. M.; Karellas, P.; Krippner, G.; Lessene, R.; Porter, C. J. H. Cationic poly-L-lysine dendrimers: pharmacokinetics, biodistribution and evidence for metabolism and bioresorption after intravenous administration in rats. *Mol. Pharmaceutics* **2006**, *3*, 614–627.

(28) Kaminskas, L. M.; Boyd, B. J.; Karellas, P.; Krippner, G. Y.; Lessene, R.; Kelly, B.; Porter, C. J. H. The impact of molecular weight and PEG chain length on the systemic pharmacokinetics of PEGylated poly-L-lysine dendrimers. *Mol. Pharmaceutics* **2008**, *5*, 449–463.

(29) Rosowsky, A.; Forsch, R.; Uren, J.; Wick, M. Methotrexate analogues, 14. Synthesis of new gamma-substituted derivatives as dihydrofolate reductase inhibitors and potential anticancer agents. *J. Med. Chem.* **1981**, *24*, 1450–1455.

(30) Taratula, O.; Garbuzenko, O. B.; Kirkpatrick, P.; Pandya, I.; Savla, R.; Pozharov, V. P.; He, H.; Minko, T. Surface-engineered targeted PPI dendrimer for efficient intracellular and intratumoral siRNA delivery. *J. Controlled Release* **2009**, *140*, 284–293.

(31) Singh, P.; Gupta, U.; Asthana, A.; Jain, N. K. Folate and folate-PEG-PAMAM dendrimers: synthesis, characterization, and targeted anticancer drug delivery potential in tumor bearing mice. *Bioconjugate Chem.* **2008**, *19*, 2239–52.

(32) Wang, S.; Lee, R. L.; Mathias, C. J.; Green, M. A.; Low, P. S. Synthesis, purification, and tumor cell uptake of 67Ga-desferoxamine-folate, a potential radiopharmaceutical for tumor imaging. *Bioconjugate Chem.* **1996**, *7*, 56–62.

(33) Kaminskas, L. M.; Boyd, B. J.; Karellas, P.; Henderson, S. A.; Giannis, M. P.; Krippner, G.; Porter, C. J. Impact of surface derivatisation of poly-L-lysine dendrimers with anionic arylsulphonate or succinate groups on intravenous pharmacokinetics and disposition. *Mol. Pharmaceutics* **2007**, *4*, 949–961.

(34) Whetstine, J. R.; Flatley, R. M.; Matherly, L. H. The human reduced folate carrier gene is ubiquitously and differentially expressed in normal human tissues: identification of seven non-coding exons and characterisation of a novel promoter. *Biochem. J.* **2002**, *367*, 629–640.

(35) Wang, Y.; Zhao, R.; Russell, R. G.; Goldman, D. Localization of the murine reduced folate carrier as assessed by immunohistochemical analysis. *Biochim. Biophys. Acta* **2001**, *1513*, 49–54.

(36) Weitman, S. D.; Lark, R. H.; Coney, L. R.; Fort, D. W.; Frasca, V.; Zurawsky, V. R. J.; Kamen, B. A. Distribution of the folate receptor GP38 in normal and malignant cell lines and tissues. *Cancer Res.* **1992**, *52*, 3396–3401.

(37) Westerhof, G. R.; Rijnboutt, S.; Schornagel, J. H.; Pinedo, H. M.; Peters, G. J.; Jansen, G. Functional activity of the reduced folate carrier in KB, MA104 and IGROV-1 cells expressing folate-binding protein. *Cancer Res.* **1995**, *55*, 3795–3802.

(38) Gangjee, A.; Jain, H. D.; Kurup, S. Recent advances in classical and non-classical antifolates as antitumor and antiopportunistic infection agents: Part I. *Anti-Cancer Agents Med. Chem.* **2007**, *7*, 524–542.